

# Purely Gain-Coupled Distributed Feedback Bragg Semiconductor Laser Emitting at 795 nm With a Wide Tunable Range

Volume 13, Number 2, April 2021

Chunkao Ruan

Yongyi Chen

Li Qin

Dezheng Ma

Peng Jia

Xia Liu

Lei Liang

Yuxin Lei

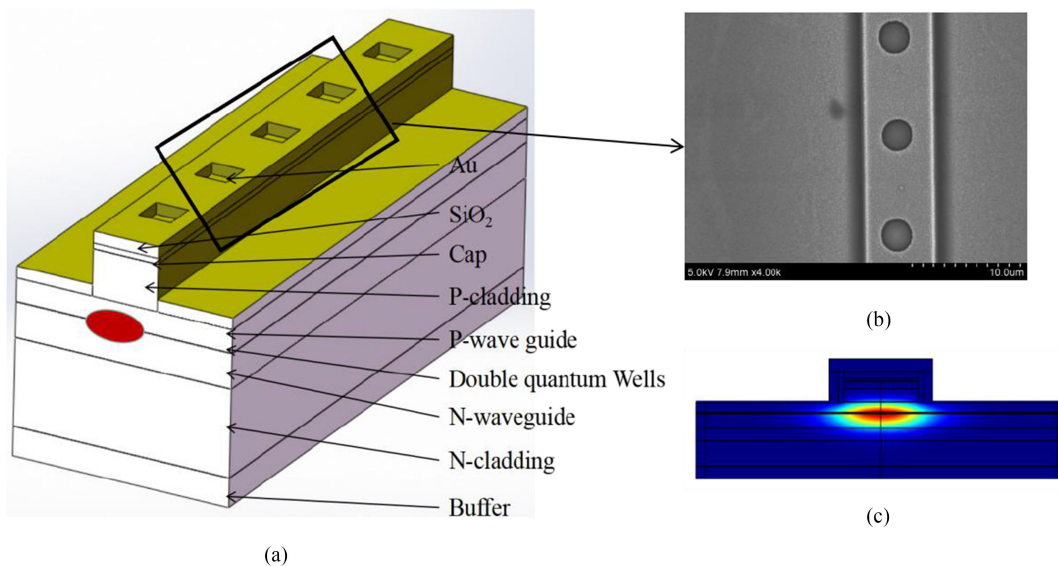
Yugang Zeng

Yue Song

Zhijun Zhang

Zaijin Li

Lijun Wang



DOI: 10.1109/JPHOT.2021.3068418

# Purely Gain-Coupled Distributed Feedback Bragg Semiconductor Laser Emitting at 795 nm With a Wide Tunable Range

Chunkao Ruan,<sup>1,2</sup> Yongyi Chen ,<sup>1</sup> Li Qin,<sup>1</sup> Dezheng Ma ,<sup>1,2</sup>  
Peng Jia,<sup>1</sup> Xia Liu ,<sup>1,2</sup> Lei Liang ,<sup>1</sup> Yuxin Lei,<sup>1</sup> Yugang Zeng,<sup>1</sup>  
Yue Song,<sup>1</sup> Zhijun Zhang,<sup>4</sup> Zaijin Li,<sup>5</sup> and Lijun Wang<sup>1,3</sup>

<sup>1</sup>State Key Laboratory of Luminescence and Application, Changchun Institute of Optics, Fine Mechanics and Physics, Chinese Academy of Sciences, Changchun 130033, China

<sup>2</sup>University of Chinese Academy of Sciences, Beijing 100049, China

<sup>3</sup>Peng Cheng Laboratory No.2, Shenzhen 518066, China

<sup>4</sup>Liaoning Institute of Science and Technology, Benxi 117004, China

<sup>5</sup>Academician Team Innovation center of Hainan Province, Key Laboratory of Laser Technology and Optoelectronic Functional Materials of Hainan Province, School of Physics and Electronic Engineering of Haikou Normal University, Haikou, Hainan 570206, China

DOI:10.1109/JPHOT.2021.3068418

This work is licensed under a Creative Commons Attribution 4.0 License. For more information, see <https://creativecommons.org/licenses/by/4.0/>

Manuscript received January 21, 2021; revised March 18, 2021; accepted March 21, 2021. Date of publication March 23, 2021; date of current version April 19, 2021. This research was funded in part by the National Science and Technology Major Project of China under Grant 2018YFB2200300; by the Frontier Science Key Program of the President of the Chinese Academy of Sciences QYZDY-SSW-JSC006; by the National Natural Science Foundation of China (NSFC) under Grants 62090051, 62090052, 62090054, 11874353, 61935009, 61934003, 61904179, 61727822, 61805236, and 62004194; by the Science and Technology Development Project of Jilin Province under Grants 20200401069GX, 20200401062GX, 20200501007GX, 20200501008GX, and 20200501009GX; by the Special Scientific Research Project of Academician Innovation Platform in Hainan Province YSPTZX202034, and by the Dawn Talent Training Program of CIOMP. Independent Innovation Project of State Key Laboratory of Luminescence and Applications SKL1-Z-2020-02. Corresponding authors: Yongyi Chen; Yugang Zeng (e-mail: chenyy@ciomp.ac.cn, zengyg@ciomp.ac.cn).

**Abstract:** We demonstrate a distributed feedback (DFB) semiconductor laser based on i-line lithography and surface periodic current injection technologies with a lasing wavelength of 795 nm, which corresponds to the D1 spectrum of Rb and has many applications with respect to alkali vapor lasers and atomic clocks. The maximum output power, side mode suppression ratio (SMSR), and single-longitudinal-mode tunable range of our device are 50.89 mW (at 20 °C), 34.56 dB, and 12.792 nm, respectively. The rate of change in wavelength with temperature of the laser is 0.401 nm/°C, which is equivalent to that of a Fabry-Perot (FP) laser and much better than that of a general DFB device. This device has a cavity the same as an FP laser without any etching gratings, meanwhile the lasing spectrum behaves a single longitudinal mode characteristic as a DFB laser.

**Index Terms:** 795 nm, distributed-feedback gain-coupled, periodic current.

## 1. Introduction

Distributed feedback (DFB) semiconductor lasers allow for stable single-longitudinal-mode lasing and have tunable wavelengths, narrow line widths, and direct modulation capability. They are widely

TABLE 1  
Epitaxial Structure of Proposed Chip

Layer	Material	Thickness(μm)	
7	GaAs	0.1	Cap
6	Al(x)GaAs	0.8	P-cladding
5	Al(x)GaAs	0.4	P-wave guide
4	Al(x)In(y)GaAs*2	0.0055	Double quantum wells
3	Al(x)GaAs	0.6	N-wave guide
2	Al(x)GaAs	1.5	N-cladding
1	GaAs	0.5	Buffer

used in optical communication [1], material processing [2], pumping source [3], and integrated optics [4]. DFB lasers can be divided into two types: index-coupled and gain-coupled [5]. The spectra of index-coupled DFB lasers, which have uniform grating periods, have an intrinsic drawback in that they feature two degenerated modes that are symmetric with respect to the Bragg frequency [5]. Although this mode degeneracy can be eliminated by applying a 1/4-wavelength phase shift grating to achieve stable single-longitudinal-mode lasing [6], this causes the carriers in the center of the laser cavity to be consumed in large quantities, resulting in a space hole burning effect at high output power [7]. In addition, phase shift grating DFB devices require complicated fabrication technologies such as secondary epitaxy, making them expensive to manufacture.

Gain-coupled DFB lasers with periodic loss or gain can also be used to obtain single-longitudinal-mode lasing [8]–[9]. Such lasers have the advantages of high single-mode yield [10], [11], insensitivity to external cavity feedback [12], narrow line widths [13], [14], and high modulation bandwidths [15], [16]. However, conventional gain-coupled DFB lasers also require complicated fabrication technologies such as secondary epitaxy [9], providing them with no cost advantages relative to index-coupled DFB lasers.

A laser with a wavelength of 795 nm, corresponding to the D1 transition line of  $^{87}\text{Rb}$ , can be applied in magnetic resonance imaging [18], rubidium vapor laser pumping [19], and rubidium atomic clocks [20]. To date, there has been little research on 795-nm DFB lasers with the exception of a single spectroscopic study carried out in 2005 [21]. It would therefore be highly useful to conduct further study on DFB laser emitting at 795 nm.

In this study, we fabricated a gain-coupled DFB device that lases at 795 nm using surface periodic electrical injection technology. The proposed device achieves the gain-coupled effect via surface periodic current injection based on i-line lithography technology without the use of complicated technologies such as secondary epitaxy or nano-scale gratings. This periodic electrical injection causes a periodic gain difference in the active quantum wells [22]–[25], enabling the proposed device to achieve stable single-longitudinal-mode lasing. At 20 °C, the maximum side mode suppression ratio (SMSR) reaches as high as 34.56 dB, and at 180 mA, the maximum power is 50.89 mW. The maximum continuous single-longitudinal-mode tunable range is 12.792 nm and the slope of the wavelength change with temperature is 0.401 nm/°C, a much better value than the less than 0.1 nm/°C typically achieved by general DFB devices [26], [27]. These characteristics give the proposed device the single-longitudinal-mode characteristics of general DFB lasers and the wide tuning performance of Fabry-Perot (FP) lasers.

## 2. Structure and Fabrication

The epitaxial structural parameters of the proposed laser are listed in Table 1. As a gain material, the device uses AlInGaAs double quantum wells. After applying metal organic chemical vapor

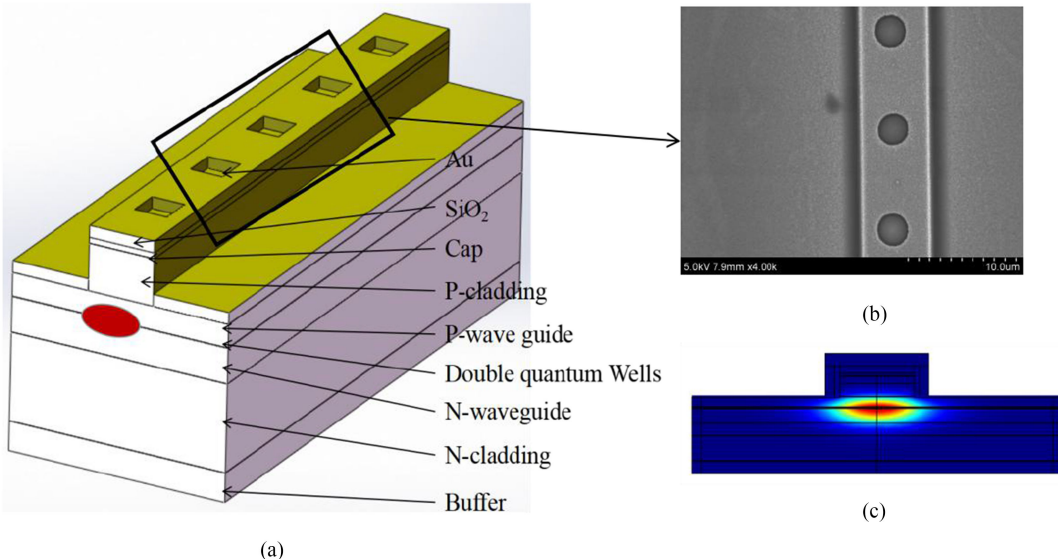


Fig. 1 (a) Device schematic. (b) Scanning electron microscope image of device. (c) Transverse-mode distribution map simulated using COMSOL Multiphysics.

deposition (MOCVD) to grow the epitaxial structure of the chip, an initial photolithography process is applied to fabricate the ridge waveguide.  $\text{SiO}_2$  is then deposited by plasma enhanced chemical vapor deposition(PECVD) to form an insulation layer, and periodic electrode windows are formed by applying photolithography directly to the insulation layer of the ridge. Metal contacts and film coating are processed as ordinary FP layers.

A schematic of the DFB laser is shown in Fig. 1(a). The active region of the device comprises double-quantum-well AlInGaAs. And after the simulation by COMSOL Multiphysics, we decided that the laser has a ridge width of  $6 \mu\text{m}$ , a period of  $8.97 \mu\text{m}$ , and an etched ridge depth of  $880 \text{ nm}$  (Fig. 1(c)), which can accommodate a single transverse mode simulated by COMSOL Multiphysics. Fig. 1(b) is the SEM image of the device. Since the width( $2 \mu\text{m}$ ) of the squares' window is very close to the resolution( $0.5 \mu\text{m}$ ) of photolithography, the squares' windows become to the circles under the diffraction effect. Periodic injections of current using surface periodic electrical injection technology cause a nonuniform distribution of carriers in the quantum wells, which in turn produces a gain contrast in the wells, as shown in Fig. 2(a). Because the device has no etched grating, it relies solely on a gain-coupled mechanism produced by the periodic current injection, which also changes the refractive index, as shown in Fig. 2(b).

In our previous paper, we derived the coupling coefficient  $\kappa$ [21] as

$$\kappa = k_0 \Gamma \left( \Delta n + i \frac{\Delta g}{4k_0} \right) \quad (1)$$

where  $\Gamma$  is the optical confinement factor of the device,  $k_0$  is the vacuum wave number corresponding to vacuum wavelength  $\lambda_0$ ,  $\Delta n$  is the change in refractive index and,  $\Delta g$  is the change in gain/loss change.

In our device,  $\Gamma = 0.0106$  (as calculated by COMSOL Multiphysics),  $\Delta n = 0.00021$  (Fig. 2(b)) and  $\Delta g = 645.186/\text{cm}$  (Fig 2(a)). Substituting these values into Equation (1), we obtain  $\kappa = 0.352 + 3.42i \text{ cm}^{-1}$ . Based on a device cavity length of  $L = 1 \text{ mm}$ , we obtain the coupling strength  $\kappa L = 0.0352 + 0.342i$ . In this relation, the real component is much smaller than the imaginary component, with a real-to-imaginary ratio of only 0.103. In addition, the coupling strength  $\kappa L$  of a conventional index-coupled DFB lasers would be greater than one [28] (with even multi-longitudinal-mode index-coupled DFB lasers attaining coupling strengths of 0.3 [29]), far exceeding the strength

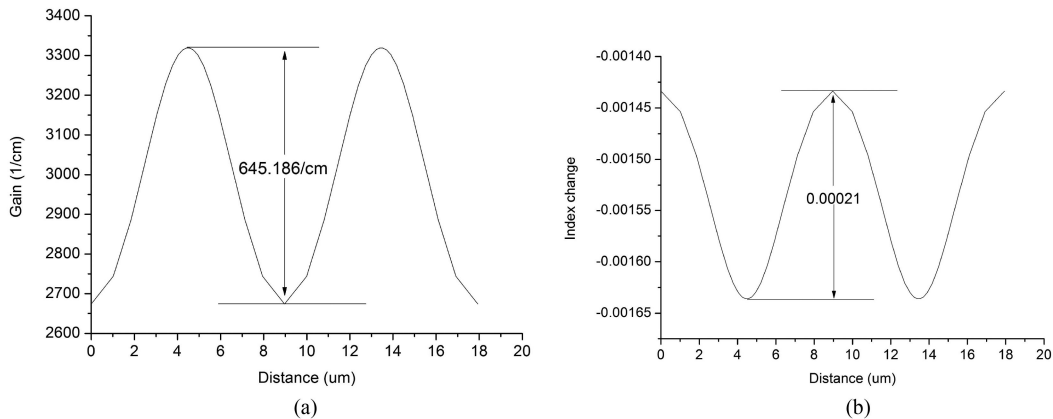


Fig. 2. (a) One-dimensional gain distribution and (b) one-dimensional index change in quantum well of pure periodic anode device without etched grating structure (both simulated using PICS3D).

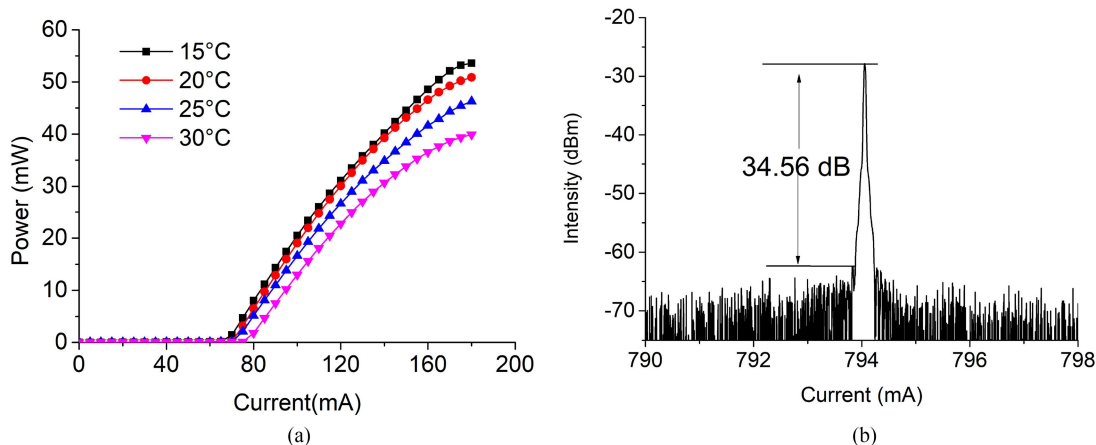


Fig. 3 (a) Current-power curve at different temperatures. (b) Typical spectrum of device at 149 mA and 20°C.

of our device. As the index-coupled effect of our device is negligible, it is a purely gain-coupled DFB laser.

### 3. Results and Discussion

Fig. 3(a) shows the current-power (CW) curves of the device at different temperatures. The length of the device cavity (which is facet-coated with 99% high-reflection and 0.5% anti-reflection materials) is 1 mm. At 20 °C, a maximum device power of 50.89 mW is achieved 180 mA. Fig. 3(b) shows a typical spectrum of the device, which has a maximum SMSR of 34.56 dB. It is seen from Fig. 3(a) that, as the temperature increases, the threshold current increases and the power at a given current decreases.

The significant increase in the threshold current with the temperature [30] is attributable to the fact that the gain coefficient of a semiconductor material depends significantly on the temperature. As the temperature increases, the occupancy rate of electrons and holes near the Fermi level becomes flatter, reducing the carrier recombination rate. Increasing the temperature also increases

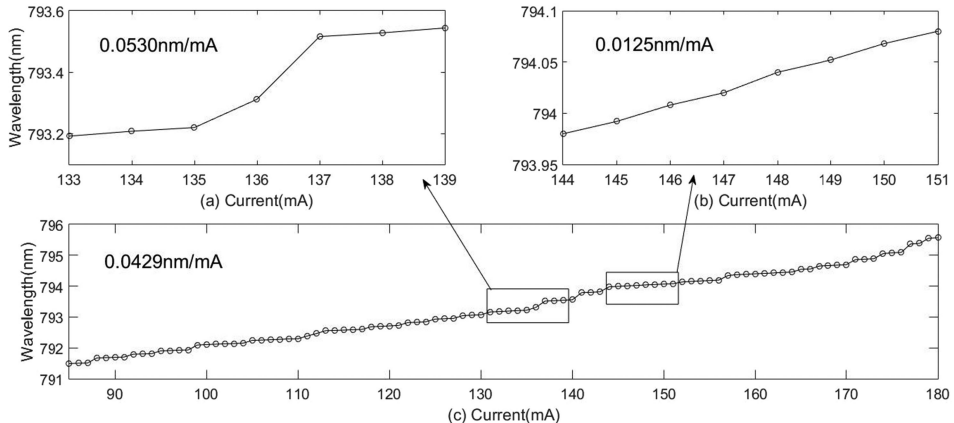


Fig. 4 Wavelength as a function of current at 20 °C.

the leakage current, which in turn reduces the gain coefficient while enhancing the absorption coefficient, thereby increasing the threshold value of the laser and decreasing its power. At low temperatures, high gain can be obtained even at reduced injected carrier concentrations because the light absorption capability of the material becomes weaker as the temperature is reduced, concentrating the injected carriers at the edge of the energy band and making it easier to achieve population inversion, thereby reducing the threshold of the laser while increasing its power.

Fig. 4 shows the wavelength as a function of current at 20 °C. It is seen from Fig. 4(c) that the overall average slope of change in wavelength with current is 0.0429 nm/mA and that the wavelength often changes relatively smoothly with current. In many regions, there is no mode hopping and the wavelength changes continuously. In the region shown in Fig. 4(b), the average rate of change is 0.0125 nm/mA. Steeper curves corresponding to mode hopping occur in the region from 135 to 137 mA (Fig. 4(a)), in which the average rate of change is 0.0503 nm/mA. As the injection current increases, the band gap in the semiconductor material decreases, the junction temperature of the heterojunction increases, and the gain spectrum of the quantum well is red shifted; all of these effects lead a redshift in the laser's wavelength. In addition, mode hopping generally does not occur in DFB lasers but often occurs in FP lasers.

The mode interval of the FP cavity is 0.092 nm. It is seen from Fig. 4(a) that increasing the current from 135 to 136 mA and from 136 to 137 mA results in wavelength changes of 0.092 and 0.204 nm, respectively, corresponding to 1 and 2.22 times the mode interval, respectively. Because no grating structure is used in the device, the cavity serves as an FP cavity when no current is injected. The gain-coupled DFB mechanism is formed by the formation of periodic current windows above the cavity. Because the gain coupling coefficient of the device is relatively small, the FP cavity apparently determines which mode is lasing; thus, the mode hopping occurring in injection current range of 135 to 137 mA in Fig. 4(a) is produced by FP modes.

Figs. 5(a) and (b) show, respectively, typical spectra of the device at 20 °C at different injected currents and at an injected current of 160 mA at different temperatures. In the 160-mA case, the SMSRs of all spectra from 15 to 35 °C are all above 30 dB. Fig. 6 shows the device wavelength as functions of current and temperature; as both increase, the lasing wavelength tends to red shift.

The redshift of the gain spectrum of the quantum well should increase with either the injection current or temperature. During testing, only the bottom of the device was in contact with the cooling source; as a result, the upper part of the device containing the chip, which is located far from the thermoelectric chip-controlled plate, still accumulated heat, which further red shifted the gain spectrum of the quantum well and increased the refractive index. All of these factors contributed to the redshift of the lasing wavelength shown in Fig. 6.

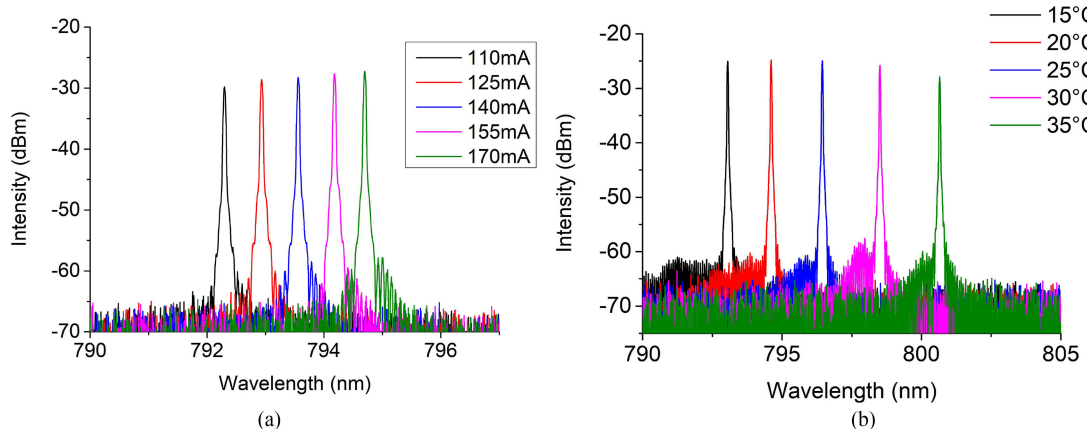


Fig. 5 (a) Wavelength spectra for different currents at 20 °C. (b) Wavelength spectra for different temperatures at 160 mA.

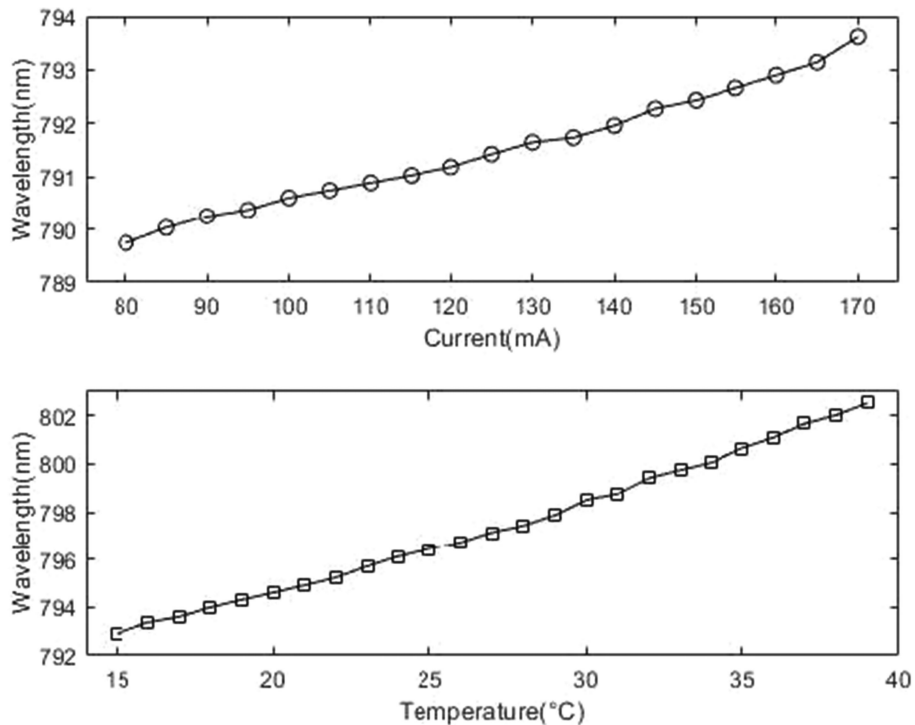


Fig. 6. Change in wavelength as a function of current (top) and temperature (bottom).

The results in Fig. 6 indicate that the maximum tunable range is 12.792 nm. This range comprises the contributions of current (3.88 nm), with an average rate of change of 0.0431 nm/mA, and temperature (9.632 nm), with an average rate of change of 0.401 nm/°C. Previously developed DFB lasers' average rates for change with temperature without mode hopping are 0.073 [26] and 0.0875 nm/°C [27], respectively. The tunable range of our device within a given temperature range is 4.58–5.49 times that of other DFB devices.

The lasing wavelength of a general DFB device is determined by the period of its Bragg grating and its effective refractive index. Although the change in the geometric size of the grating period with temperature can be ignored, the effective refractive index is, to a certain extent, temperature-dependent. Because this dependency is linear, the rate of change in the lasing wavelength of the device with temperature will be less than  $0.1 \text{ nm}^{\circ}\text{C}$  [26], [27]. Our device differs in terms of its thermal characteristics because it has a relative small gain-coupled coefficient of only  $3.42 \text{ cm}^{-1}$ , as compared to other complex-coupled DFB devices, for which the value is above  $10 \text{ cm}^{-1}$  [26]. The gain-coupled effect aids in the selection of an FP mode from among the existing modes for enabling single-longitudinal-mode lasing. Thus, when the temperature changes the lasing wavelength changes from that characteristic of the current FP mode to that of the adjacent FP mode. This continuous tuning increases the rate of change in temperature to approximately  $0.4 \text{ nm}^{\circ}\text{C}$  [31]. As a result, our device has the single-longitudinal-mode lasing characteristics of a general DFB device combined with the wide tuning performance of an FP laser.

#### 4. Conclusion

In this study, we demonstrated a tunable, purely gain-coupled DFB device with a lasing wavelength of 795 nm. The fabrication of the device requires only simple i-line lithography and periodic electrical injection technology and avoids the use of complicated or high-cost fabricating technologies such as secondary epitaxy and nano-scale gratings. As a result, our device is simpler to manufacture and cheaper than conventional DFB devices. The proposed device has a maximum SMSR of 34.56 dB and a maximum tunable single-longitudinal-mode lasing range of 12.792 nm. The rate of change of wavelength with temperature is  $0.401 \text{ nm}^{\circ}\text{C}$ , which is equivalent to that of an FP laser and much larger than that of a general DFB device. These qualities show that our lasers not only have the single-longitudinal-mode lasing characteristics of general DFB devices, but also have the wide tuning performance of FP lasers.

---

#### References

- [1] S. P. Najda *et al.*, "Lateral grating DFB AlGaN laser diodes for optical communications and atomic clocks," *J. Phys. Conf. Ser.*, vol. 810, no. 1, 2017, Art. no. 012053.
- [2] E. A. Zibik *et al.*, "High power single-mode DFB laser diodes for 10xx nm spectral range," in *Proc. IEEE Semicond. Laser Conf.*, San Diego, CA, USA, 2012, pp. 44–45.
- [3] O. Brox *et al.*, "Distributed feedback lasers in the 760 to 810 nm range and epitaxial grating design[J]," in *Semicond. Sci. Technol.*, vol. 29, no. 9, 2014, Art. no. 095018.
- [4] Z. Zhou, B. Yin, J. Michel, and J. Michel, "On-chip light sources for silicon photonics[J]," *Light-Spi. Appl.*, vol. 4, no. 11, 2015.
- [5] H. Kogelnik and C. V. Shank, "Coupled-Wave theory of distributed feedback Lasers[J]," *J. Appl. Phys.*, vol. 43, no. 5, pp. 2327–2335, 1972.
- [6] H. Soda, Y. Kotaki, H. Sudo, H. Ishikawa, S. Yamakoshi, and H. Imai, "Stability in single longitudinal mode operation in GaInAsP/InP phase-adjusted DFB lasers[J]," *Quantum Electron. IEEE J.*, vol. 23, no. 6, pp. 804–814, 1987.
- [7] S. L. Chuang, *Physics of Photonic Devices*. Hoboken, NJ, USA: Wiley, 2009, pp. 493–500.
- [8] Y. Luo, Y. Nakano, K. Tada, T. Inoue, H. Hosomatsu, and H. Iwaoka, "Purely gain-coupled distributed feedback semiconductor lasers[J]," *Appl. Phys. Lett.*, vol. 56, no. 17, pp. 1620–1622, 1990.
- [9] Y. Luo and Y. Nakano, "Fabrication and characteristics of gain-coupled distributed feedback semiconductor lasers with a corrugated active layer[J]," *Quantum Electron. IEEE J.*, vol. 27, no. 6, pp. 1724–1731, 1991.
- [10] G. P. Li and T. Makino, "Single-mode yield analysis of partly gain-coupled multiquantum-well DFB lasers [J]," *IEEE Photon. Technol. Lett.*, vol. 5, no. 11, pp. 1282–1284, Nov. 1993.
- [11] G. P. Li, T. Makino, R. Moore, N. Puetz, K. W. Leong, and H. Lu, "Partly gain-coupled 1.55  $\mu\text{m}$  strained-layer multiquantum-well DFB lasers[J]," *IEEE J. Quantum Electron.*, vol. 29, no. 6, pp. 1736–1742, Jun. 1993
- [12] R. Hui and M. Kavehrad, "External feedback sensitivity of partly gain-coupled DFB semiconductor lasers[J]," *IEEE Photon. Technol. Lett.*, vol. 6, no. 8, pp. 897–899, Aug. 1994.
- [13] K. Kudo, J. I. Shim, K. Komori, and S. Arai, "Reduction of effective linewidth enhancement factor alpha of DFB lasers with complex coupling coefficients [J]," *IEEE Photon. Technol. Lett.*, vol. 4, no. 6, pp. 531–534, Jun. 1992.
- [14] H. Lu, G. P. Li, and T. Makino, "Spectral linewidth reduction in partly gain-coupled 1.55  $\mu\text{m}$  strained multiple quantum-well distributed feedback laser [J]," *Appl. Phys. Lett.*, vol. 63, no. 5, pp. 589–591, 1993.
- [15] A. J. Lowery and D. Novak, "Enhanced maximum intrinsic modulation bandwidth of complex-coupled DFB semiconductor lasers [J]," *Electron. Lett.*, vol. 29, no. 5, pp. 461–463, 1993.

- [16] H. Lu, G. P. Li, and T. Makino, "High-speed performance of partly gain-coupled 1.55- $\mu$ m strained-layer multiple-quantum-well DFB lasers[J]," *IEEE Photon. Technol. Lett.*, vol. 5, no. 8, pp. 861–863, Aug. 2002.
- [17] W. F. Krupke, R. J. Beach, V. K. Kanz, and S. A. Payne, "Resonance transition 795-nm rubidium laser," *Opt. Lett.*, vol. 28, no. 23, pp. 2336–2338, 2003.
- [18] B. V. Zhdanov and R. J. Knize, "Alkali lasers for magnetic resonance imaging[J]," *centr.eur.j.phys.*, vol. 8, pp. 184–193, 2010.
- [19] B. V. Zhdanov, A. Stooke, G. Boyadjian, A. Voci, and R. J. Knize, "Rubidium vapor laser pumped by two laser diode arrays," *Opt. Lett.*, vol. 33, no. 5, pp. 414–415, 2008.
- [20] G. Tandoi *et al.*, "Passively mode-locked semiconductor laser for coherent population trapping in 87Rb[C]," in *Proc. IEEE Conf. Lasers Electro-Opt. Eur., 12th Eur. Quant. Electronics. Conf. (CLEO EUROPE/EQEC)*, Munich, Germany 2011, p. 1.
- [21] D. Slavov, C. Affolderbach, and G. Milet, "Spectral characterisation of tuneable narrow-band diode lasers for Rb atomic spectroscopy and precision instruments," in *Proc. SPIE 5830, 13th Int. School Quant. Electron.: Laser Phys. Appl.*, 22 Apr. 2005, pp. 281–285.
- [22] F. Gao *et al.*, "Study of gain-coupled distributed feedback laser based on high order surface gain-coupled gratings[J]," *Opt. Commun.*, vol. 410, pp. 936–940, 2017.
- [23] Y. X. Lei *et al.*, "High-power single-longitudinal-mode double-tapered gain-coupled distributed feedback semiconductor lasers based on periodic anodes defined by i-line lithography," *Opt. Commun.*, vol. 443, pp. 150–155, 2019.
- [24] Y. X. Lei *et al.*, "990 nm High-Power high-beam-quality DFB laser with narrow linewidth controlled by gain-coupled effect[J]," *IEEE Photon. J.*, vol. 11, no. 1, Feb. 2019, Art. no. 1500609.
- [25] Y. X. Lei *et al.*, "996 nm high-power single-longitudinal-mode tapered gain-coupled distributed feedback laser diodes," *Appl. Opt.*, vol. 58, no. 23, pp. 6426–6432, 2019.
- [26] N. Chen, A. Kitamoto, Y. Nakano, and K. Tada, "Chirped-grating tunable DFB laser: Novel laser diode with broader continuous tuning range[J]," in *Proc. SPIE - Int. Soc. Opt. Eng.*, 1993, pp. 347–350.
- [27] L. Y. Li *et al.*, "Experimental demonstration of a low-cost tunable semiconductor DFB laser for access networks[J]," in *Semicond. Sci. Technol.*, 2014, vol. 29, no. 9, Art. no. 095002.
- [28] K. David, G. Morthier, P. Vankwikelberge, R. G. Baets, T. Wolf, and B. Borchert, "Gain-coupled DFB lasers versus index-coupled and phase shifted DFB lasers: A comparison based on spatial hole burning corrected yield," *IEEE J. Quantum Electron.*, vol. 27, no. 6, pp. 1714–1723, Jun. 1991.
- [29] J. Decker, P. Crump, J. Fricke, A. Maassdorf, G. Erbert, and G. Trankle, "Narrow stripe broad area lasers with high order distributed feedback surface Gratings," *IEEE Photon. Technol. Lett.*, vol. 26, no. 8, pp. 829–832, Apr. 2014.
- [30] I. Hayashi, M. B. Panish, and F. K. Reinhart, "GaAs-Al<sub>x</sub>Ga<sub>1-x</sub>As double heterostructure injection Lasers[J]," *J. Appl. Phys.*, vol. 42, no. 5, pp. 1929–1941, 1971.
- [31] A. Fujiwara *et al.*, "Temperature-dependence of lasing spectrum for TlInGaAs/InP DH laser diodes and 77K CW operation[C]," in *Proc. IEEE Int. Conf. Indium Phosphide Related Mater.*, 2003, Santa Barbara, CA, USA, 2003, pp. 96–99.